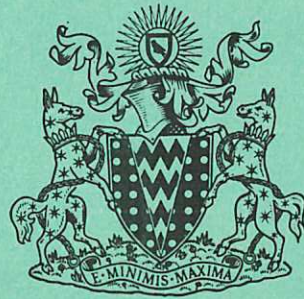
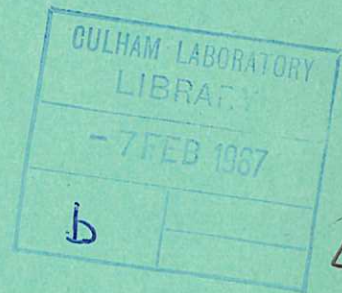


This document is intended for publication in a journal, and is made available on the understanding that extracts or references will not be published prior to publication of the original, without the consent of the author.



United Kingdom Atomic Energy Authority  
RESEARCH GROUP  
Preprint

# THE TRAJECTORIES OF MAGNETIC FIELD LINES IN TOROIDAL STELLARATORS

A. GIBSON

Culham Laboratory  
Abingdon Berkshire

1967

CLM-P 129

Enquiries about copyright and reproduction should be addressed to the Librarian, UKAEA, Culham Laboratory, Abingdon, Berkshire, England

THE TRAJECTORIES OF MAGNETIC FIELD LINES IN  
TOROIDAL STELLARATORS

by

A. GIBSON

(Submitted for publication in Phys. Fluids)

A B S T R A C T

Computations are presented to show that in a toroidal  $\ell = 3$  stellarator, in addition to the well known inward shift of the magnetic axis, the following effects occur: the rotational transform on the last closed surface is substantially less than the winding transform; the closed and open surfaces are separated by a complex region; the shape of the surfaces in the central region is essentially as predicted by Aleksin. The maximum shear available in a feasible stellarator is estimated and compared to that required for stability. The effect of perturbations on the perfect toroidal system is computed.

U.K.A.E.A. Research Group,  
Culham Laboratory,  
Abingdon,  
Berks.

December, 1966. (ED)

## C O N T E N T S

	<u>Page</u>
1. INTRODUCTION	1
2. NOMENCLATURE AND NUMERICAL PROCEDURE	2
3. A STRAIGHT SYSTEM WITH HELICAL SYMMETRY	3
4. THE EFFECTS OF TOROIDICITY	4
5. THE EFFECT OF ADDING A VERTICAL FIELD	6
6. THE EFFECT OF PERTURBATIONS ON THE PERFECT TOROIDAL SYSTEM	7
7. DISCUSSION	8
8. CONCLUSIONS	9
9. ACKNOWLEDGEMENTS	10
10. REFERENCES	11

## 1. INTRODUCTION

The concept of plasma confinement in toroidal stellarator systems<sup>(1)</sup> is based upon the idea that the conductor configuration generates lines of force which lie on a set of closed, nested, toroidal magnetic surfaces. The existence of these surfaces is not proved theoretically or experimentally and examples have been given<sup>(2,3)</sup> of helical stellarator fields which do not have such surfaces.

The existence of magnetic surfaces can be proved<sup>(4)</sup> in straight systems with perfect helical symmetry and Kruskal<sup>(5)</sup> has proved that closed surfaces exist in any rotational transform system in which the transform per field (see Section 3) is infinitesimally small. Green and Johnston<sup>(6)</sup> have shown that, in toroidal stellarators produced by helical currents flowing on the surface of a torus, a nest of closed magnetic surfaces exists, in the asymptotic sense, when the toroidicity and the rotational transform per field period are infinitesimally small. The nest is centered on a magnetic axis which is displaced towards the major axis from the centre of the helical surface currents. Aleksin<sup>(7)</sup> has examined the region near the magnetic axis for the case of filaments wound on the surface of a torus: he shows that in the limit of small pitch and small aspect ratio the magnetic axis splits and an inner separatrix appears. Melnikov<sup>(8)</sup> treats the separatrix region approximately showing that, while toroidal effects reduce the volume of closed surfaces, some correction of this reduction can be achieved by adding an appropriately directed vertical field.

In the past, stellarators<sup>(9)</sup> have been constructed with relatively small toroidicity and rotational transform per field period: however recent theoretical criteria for stability<sup>(10)</sup> require either high shear or an average magnetic well or both<sup>(11)</sup>. In order to obtain configurations of this type we are led to use the high shear in the separatrix region and to choose systems with considerable toroidicity; approximate treatments of the problem of magnetic surfaces are not available for these conditions.

This paper describes a computer study of the trajectories of magnetic field lines in  $\ell = 3$  toroidal stellarator fields generated by filamentary conductors.

The limiting transform on the last closed surface is obtained as a function of aspect ratio and is related to the shear necessary for stabilization of universal instabilities. The effect of various perturbations on the basic field system is examined. Numerical errors and the availability of computer time limit the investigations to, typically, 160 field periods or 20 transits around the torus. Surfaces, which in these computations appear closed, may well be revealed to be open by more extensive integration; we cannot therefore establish the existence or otherwise of closed magnetic surfaces. To establish confidence in the computer code it has been used to examine an analytic case with straight helical symmetry; results for this system (which are well known) are included in Section 3 for comparison with the toroidal system. In both systems the field lines have a compound helical structure.

## 2. NOMENCLATURE AND NUMERICAL PROCEDURE

The co-ordinate systems used are shown in Fig.1:  $(R, \theta, Z)$  are cylindrical polar co-ordinates,  $Z$  is the major axis of the torus;  $(r, \phi)$  are polar co-ordinates in the planes  $\theta = \text{const}$ , and are centred on the circular axis of the torus. The stellarator field is taken to consist of:

(a) a toroidal field

$$B_{\theta} = B_0/R \quad \dots (1)$$

where  $B_0$  is a constant.

(b) a field produced by  $2\ell$  ( $\ell = 3$ ) filamentary conductors of alternate polarity, each composed of a number of short straight sections whose ends lie on the toroidal helices

$$\begin{aligned} r &= s = \text{constant} \\ \phi &= n\theta + \alpha \end{aligned} \quad \dots (2)$$

where  $\alpha$  is a constant for each helix and is chosen to make the wires equally spaced in  $\phi$ .  $n$  is a constant defining the angular extent of a winding period ( $= \frac{2\pi}{n}$ ). In one winding period the field pattern is repeated  $\ell$  times so that the angular extent of a field period is  $\frac{2\pi}{\ell n}$ . We shall call this winding the  $\ell$ -winding.  $R_0$  is the major radius of the  $\ell$ -winding and  $R_0/s$  the aspect ratio.

The field lines are obtained by integrating the field equations

$$\frac{dR}{B_R} = \frac{R \cdot d\theta}{B_\theta} = \frac{dZ}{B_Z} \quad \dots (3)$$

step by step using a predictor-corrector method. The numerical accuracy has been estimated both by varying the integration step and by integrating backwards from a computed point towards the starting point.

### 3. A STRAIGHT SYSTEM WITH HELICAL SYMMETRY

An example of such a system is

$$\begin{aligned} B_r &= r^{\ell-1} \sin(\ell\phi - kz) \\ B_\phi &= r^{\ell-1} \cos(\ell\phi - kz) \\ B_z &= 1.0 \end{aligned} \quad \dots (4)$$

where  $(r, \phi, z)$  are cylindrical polar co-ordinates,  $\ell$  is an integer and  $k$  a constant. Similar fields but having many harmonics, are generated by  $2\ell$  filamentary conductors wound in equally spaced helices of pitch length  $\frac{2\pi\ell}{k}$  on the surface of a cylinder, adjacent helices carrying oppositely directed current. The axis of the cylinder is a field line of the system and is the magnetic axis; at small radius the magnetic surfaces are closed about this axis, while at larger radii the surfaces pass around the wires. The region of surfaces closed about the magnetic axis is separated from the region where surfaces pass outside the wires by a limiting surface, the separatrix. The field lines in the inner region of such a system with  $\ell = 3$  lie on surfaces whose cross sections ( $z = \text{constant}$ ) are distorted triangles which rotate as we move along the  $z$  axis. The field lines also rotate but less quickly than the triangles; consequently the field lines have two characteristic helical periods, one associated with the rotation of the triangle and one with their own motion around the triangle. A field line then, has the form of a helix wound on a cylinder, which itself has a helical axis encircling the magnetic axis. The direction of rotation of a field line about the magnetic axis oscillates, but there is a net average rotation. The rotation/field period, averaged over many field periods is known as the rotational transform

per field period ( $\iota_k$ ). The projection of the field line on a plane  $z = \text{constant}$  has a cycloidal form (see Fig.11).

Computed surfaces in the field (4) for  $\ell = 3, k = 2$  are shown in Fig.2, where the surfaces are obtained by plotting the field line intersections with the planes

$$z = n\pi ; \quad n = 0, 1, 2, 3 \dots \dots \dots \quad \dots (5)$$

In this case we expect the transform in the last closed surface (separatrix) to be equal to the 'winding transform', i.e.  $\iota_k = 120^\circ/\text{field period}$ . The rate of increase of transform becomes infinite as we approach the separatrix and the step length necessary to integrate accurately along a field line becomes very short. Consequently the transform on the last closed surfaces which could be followed numerically was  $106^\circ/\text{field period}$ , but the computed variation of transform with radial distance from the theoretical separatrix was in agreement with asymptotic theory<sup>(12)</sup>.

#### 4. THE EFFECTS OF TOROIDICITY

Fig.3 shows the results of computations in a toroidal  $\ell = 3$  case with an aspect ratio at the  $\ell$ -winding of 2.8 (6.7 at the separatrix), 8 field periods in the circumference of the torus and a mean winding pitch angle of  $45^\circ$ . In this case the diagram is an R-Z plot of the intersections of the field lines with the planes

$$\theta = p \cdot \left(\frac{2\pi}{m}\right) \quad \dots (6)$$

$$p = 0, 1, 2, 3 \dots \dots \dots$$

$m = \text{number of field periods in the circumference} (= 3n \text{ in equation (2)}).$

An inward displacement from the centre of the  $\ell$ -winding ( $R = 0.3 \text{ m}$ ) is evident. The central structure is similar to that predicted by Aleksin<sup>(7)</sup> and the axes obtained by him are shown for comparison. This structure occurs in a region where the rotational transform is extremely small ( $\iota_k < 1.25^\circ$ ). The transform per field period on the last closed surface is much less than  $120^\circ$ . In this case the last



closed surface is the one on which the local rate of rotation of the field line just equals the rate of rotation of the adjacent wire; at larger aspect ratios the surfaces break open before the rotation is as rapid as this.

In the toroidal case we find there is no well defined separatrix; rather there is a separatrix region where the field line trajectories lie on complex interlaced surfaces. This behaviour is similar to that predicted by Melnikov<sup>(8)</sup>. An example is shown in Fig.4 which is an outer surface of Fig.3. The error is less than 0.01 mm over the complete trajectory and less than 0.002 mm over the first 14 field periods, at which point the complex structure is already apparent. The thickness of the separatrix region, from a surface which appears closed when computed through 160 field periods to the region where no surfaces enclose the magnetic axis, is  $\sim 1.5$  mm or  $\sim 3\%$  of the separatrix radius.

The existence of these complex surfaces, which we find to be open after 1 to 2 transits around the minor circumference (15  $\rightarrow$  20 field periods), raises the question of whether the inner surfaces which appear closed in 10 transits around the minor circumference are in fact closed or whether more extensive integration would show that all the surfaces in a toroidal system are complex.

The value of  $\iota_k$  (max) for a number of windings with the same pitch angle ( $\sim 45^\circ$ ) but various aspect ratios ( $R_0/s$ ) is shown in Fig.5. The minor radius ( $s$ ) of the  $\ell$ -winding, the  $\ell$ -winding current and the toroidal magnetic field ( $B_\theta$ ), are the same throughout the figure except for points with  $R_0/s = 4.4$  and  $5.0$ . The ratio  $r_m/s$  ( $r_m$  = maximum radius of last closed surface) increases with  $R_0/s$  in the range  $0.41 \rightarrow 0.46$ . The last closed surface is established to be closed after 40 field periods for  $R_0/s < 5$ , for 20 field periods at  $R_0/s = 13$  and for 10 field periods for all other points. For  $R_0/s < 30$  the computation has been made using the field of the complete  $\ell$ -winding; for  $R_0/s > 30$  the field lines have been computed through the centre 10 field periods of a winding of total extent 50 field periods. The upper limit indicated for  $\iota_k$  is obtained by calculating, by extrapolation, what the rotational transform would be at the first open surface computed. At

aspect ratios  $< 30$ , we have verified that the segmentation of the  $\ell$ -winding does not affect the results by varying the number of segments and by comparison with a case (with different winding pitch) where the  $\ell$ -winding consists only of circular loops (the generating circles of a torus).

We see from Fig.5 that  $\iota_k = 30^\circ/\text{field period}$  at small aspect ratio and that it increases only very slowly with  $R_0/s$ . Increasing the aspect ratio above 5000 produces no further increase in  $\iota_k$ , (beyond  $\sim 82^\circ$ ) and we presume that some asymmetry other than toroidicity is responsible for this. Possibilities are the finite segment length used to calculate the field of the  $\ell$ -winding and the fact that only 50 field periods of winding are used for these large aspect ratios. Thus we see that for practical stellarators ( $R_0/s < 8$ ) with a winding pitch angle of  $45^\circ$  the maximum obtainable transform is only  $30^\circ/\text{field period}$ . To obtain a substantial increase to  $60^\circ/\text{field period}$  it is necessary to have an aspect ratio at the  $\ell$ -winding of  $R_0/s \sim 30$ . The limiting transform is essentially unchanged when the  $\ell$ -winding filaments are each replaced by three equally spaced filaments carrying the same total current and spread over  $20^\circ$  of minor circumference. The limiting transform is somewhat increased for less steeply pitched windings and for smaller  $r_m/s$ ; thus for pitch angle of  $17^\circ$  and  $r_m/s = 0.22$  we find  $\iota_k (\text{max}) \sim 36^\circ$  for  $R_0/s = 3$ .

##### 5. THE EFFECT OF ADDING A VERTICAL FIELD

Fig.6 shows the effect of adding a vertical field ( $B_z$ ) to the configuration of Fig.3 in order to give the average magnetic well configuration proposed by Taylor<sup>(11)</sup>. The volume of closed surfaces is reduced and the outer surfaces are serrated. Fig.7 shows the effect of an oppositely directed vertical field. In this case the volume of closed surfaces is increased and the transform on the last closed surface is substantially increased to  $51^\circ$  ( $2\pi/7$  radians)/field period, as predicted qualitatively by Melnikov<sup>(13)</sup>. In both cases the region near the magnetic axis has distorted elliptical surfaces and the rotational transform is approximately independent of radius. In the central region near  $R = 0.3$  m, where the

$\ell$ -winding field is weak, the field line trajectories are determined in a simple way by the vertical and toroidal fields.

Fig.8 shows the variation with  $R$  of  $\iota_k$  and of  $V'$ , the volume/unit flux; this quantity is obtained by evaluating

$$V' = L t \frac{B_\theta (R = R_0)}{R_0 \cdot \alpha} \int_0^{\theta=\alpha} \frac{d\ell}{B}$$

where the integral is evaluated along the field line. An approximate estimate of the well depth<sup>(11)</sup>,  $\frac{2\delta}{R_0}$  ( $\delta$  = displacement of nest centre from winding centre) is indicated, together with the computed value. Fig.8 presents results for the configurations of Figs.3, 6 and 7 and for a case with larger aspect ratio. At the larger aspect ratio, with  $B_z = 0$ ,  $V'$  shows little variation with  $R$ , but at the smaller aspect ratio, due to the toroidal displacement, there is a pronounced average magnetic well. In the cases with vertical field, the small shear region may extend over all the closed surfaces, or, depending on the magnitude of the vertical field, it may be bounded by a region of large shear. The quantity  $V'$  varies smoothly over the region of the well.

## 6. THE EFFECT OF PERTURBATIONS ON THE PERFECT TOROIDAL SYSTEM

Very small mechanical errors in the construction of a real  $\ell$ -winding can affect the structure of the field. The effect of giving the  $\ell$ -winding minor radius an  $m = 0$  ripple with the same period as the winding itself (we shall call such perturbations resonant) is shown in Fig.9. The ripple amplitude is 1/2000 of the  $\ell$ -winding radius. In the unperturbed field the field line escapes due to the build up of numerical errors after 110 field periods (error  $\sim 0.8$  mm). In the perturbed field the line escapes after only 48 field periods (error  $\sim 0.03$  mm) and the surface is complex. Similar calculations show the perturbation has no detectable effect on the surfaces well inside the separatrix; for example a surface with  $\iota_k = 16^0$  is not affected in 160 field periods.

The effect of a larger resonant perturbation is shown in Fig.10 for configurations of Fig.3 and Fig.6. The perturbation is produced by circular loops of

alternate polarity in R-Z planes at each field period. The system produces a 7% modulation of  $B_\theta$  and introduces a periodic  $B_R$  of up to 2.4% of  $B_\theta$ . The outer surfaces become complex and open; the innermost surfaces are not affected in the case with vertical field and are modified but still closed with no vertical field. Similar results were obtained for a perturbation of the same magnitude produced by a single coil in one cross section.

## 7. DISCUSSION

The maximum transform found in Section 4 implies a maximum attainable shear. Kadomtsev and Pogutse<sup>(10)</sup> give a criteria for stabilization of the universal drift mode of instability in a one dimensional plasma. It is:-

$$\frac{\rho}{L_S} > \left(\frac{m}{M}\right)^{1/2} \quad \dots (8)$$

where  $\rho$  is the density gradient length,  $L_S$  the shear length,  $m$  and  $M$  the electron and ion masses.

We can obtain a typical value in our case by taking

$$\rho = r_m$$

and

$$L_S = \frac{L_K}{\iota_K}$$

where  $L_K$  = the length of a field period. For a mean winding pitch angle of  $45^\circ$ ,  $r_m = \frac{S}{2}$  and  $\iota_K$  (max) =  $\pi/6$  (see Fig.5), we obtain:-

$$\frac{\rho}{L_S} = \frac{1}{8}$$

which easily satisfies equation (8). The influence of the maximum attainable shear on plasma confinement is discussed elsewhere<sup>(14)</sup>.

We do not find any simple structure associated with the magnetic surfaces in either the pure toroidal fields or in the perturbed cases, whereas others<sup>(15,16)</sup> have reported chain and island structures. We have particularly looked for such structures on surfaces where the total rotational transform is a submultiple of  $360^\circ$ . The reason for this lack of structure can be inferred from Fig.11 which shows a part of the trajectory of one of the field lines of Fig.3 in the R-Z plane.

This plot shows, as is well known, that the rotation of the field line about the magnetic axis is not monotonic and at such points as 'A' is actually opposed to the twist of the winding. Consequently even when the total transform is a sub-multiple of  $360^\circ$  such a field line does not remain in phase with perturbations such as the ones we have considered: thus we would not expect the appearance of a simple structure. We would expect such a structure for perturbations localised to small regions of the major circumference when the transform is such that the field line always passes through the region at the same minor azimuth ( $\phi$ ). Kerst<sup>(16)</sup> has demonstrated that large islands occur in this case. Similarly we expect this structure if a helical perturbation such as equations (4) and (5) is applied to a system with a first order rotational transform such as is produced by a uniform  $B_z$  and a straight current-carrying rod along the  $z$  axis. Computation of this case shows well-developed chains, at certain radii, in agreement with the predictions of analytic theory.

## 8. CONCLUSIONS

The most important effect revealed in these computations is that toroidicity in sheared stellarator systems severely reduces the maximum transform (Fig.5) and hence limits the obtainable shear. In practicable systems the shear is sufficient to give a mean value of  $\frac{\rho}{L_S}$  of  $\frac{1}{8}$  compared to the value of  $1/43$  necessary to stabilise the universal drift mode in a slab model of a hydrogen plasma<sup>(10)</sup>. Very small (1 part in 2000) resonant mechanical errors in the helical winding can reduce this limiting transform still further. Field errors of the order of 2 to 7% either resonant or localised near one cross section can cause the majority of the surfaces to open.

The addition of a vertical field produces an average magnetic well or anti-well as predicted by Taylor<sup>(11)</sup>. The region near the magnetic axis in this case has small shear and finite rotational transform (Fig.8). For a suitable choice of vertical field this region can be surrounded by an annular region of strong shear. The vertical field which is in such a direction as to produce a mean anti-well also

leads to an increase in the volume of closed surfaces (Fig.7) and in the rotational transform on the last closed surface (Fig.8). The occurrence of complex surfaces (Fig.4) indicates that some caution is necessary in interpreting the computations; thus the inner surfaces, which appear closed when integrated to a numerical limit of 160 field periods or 20 transits around the torus, may well be revealed open by more extensive integration. The rapid improvement in closure as we move inwards through the separatrix region (see Section 4), together with Kruskal's result<sup>(5)</sup> that the error in closure of a surface decreases more rapidly than any power of  $(\frac{l_k}{2\pi})$ , give good grounds for supposing that there will be a very high degree of confinement of field lines in the inner region. Clearly, however, further investigation is needed to prove that field lines lie on nested surfaces for the  $10^5$  to  $10^7$  transits envisaged for confinement of a thermonuclear plasma.

#### 9. ACKNOWLEDGEMENTS

The author is grateful to Drs R.J. Bickerton, R.S. Pease and J.B. Taylor for many helpful discussions, to F.M. Larkin for providing the magnetic field and integration subroutines, to Miss M. Rankin for assistance with the coding, and to Miss B.A. Cheyne and the Culham Laboratory Computer Group for reliable data processing and operation of the KDF-9 computer.

## 10. REFERENCES

1. SPITZER, L. Jr. Phys. Fluids, 1, 253 (1958).
2. GEL'FAND, I.M., GRAEV, M.I., ZUEVA, N.M., MIKHAILOVA, M.S. and MOROZOV, A.I., Sov. Phys - Doklady. 7, 223 (1962).
3. MOROZOV, A.I. and SOLOV'EV, L.S., Sov. Phys - JETP. 18, 660 (1964).
4. JOHNSON, J.L., OBERMAN, C.R., KULSRUD, R.M. and FRIEMAN, E.A., Princeton University. Washington, OTS, NYO-7904 (1957).
5. KRUSKAL, M.D., Princeton University. NYO-998 (1952).
6. GREENE, J.M. and JOHNSON, J.L., Phys. Fluids. 4, 875 (1961).
7. ALEKSIN, V.F., Proc. 3rd Conference on Plasma Physics and Problems of Controlled Thermonuclear Fusion, Kharkov, 1962, 216.
8. MEL'NIKOV, V.K., Sov. Phys - Doklady. 7, 502 (1962).
9. SINCLAIR, R.M., YOSHIKAWA, S., HARRIES, W.L. and KESSLER, J.O., Phys. Fluids. 6, 937 (1963).
10. KADOMTSEV, B.B. and POGUTSE, O.P., Proc. IAEA Conference on Plasma Physics and Controlled Nuclear Fusion Research, Culham, 1965, 1, 365 (1966).
11. TAYLOR, J.B., Phys. Fluids. 8, 1203 (1965).
12. TAYLOR, J.B. and McNAMARA, B., Culham Laboratory. Private communication.
13. MEL'NIKOV, V.K., Sov. Phys - Doklady. 8, 362 (1963).
14. BICKERTON, R.J. and GIBSON, A., Phys. Fluids (To be published).
15. ZUEVA, N.M., MIKHAILOVA, M.S. and MOROZOV, A.I., Sov. Phys - Doklady. 8, 1185 (1964).
16. KERST, D.W., J. Nucl. Energy Pt C. 4, 253 (1962).





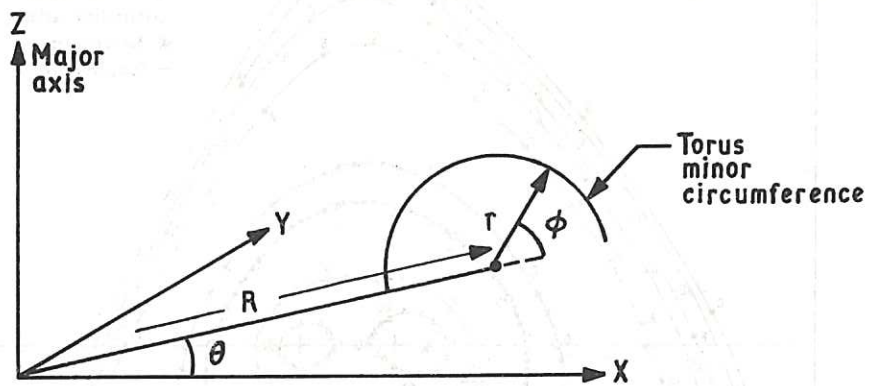


Fig. 1 Co-ordinate system (CLM-P 129)

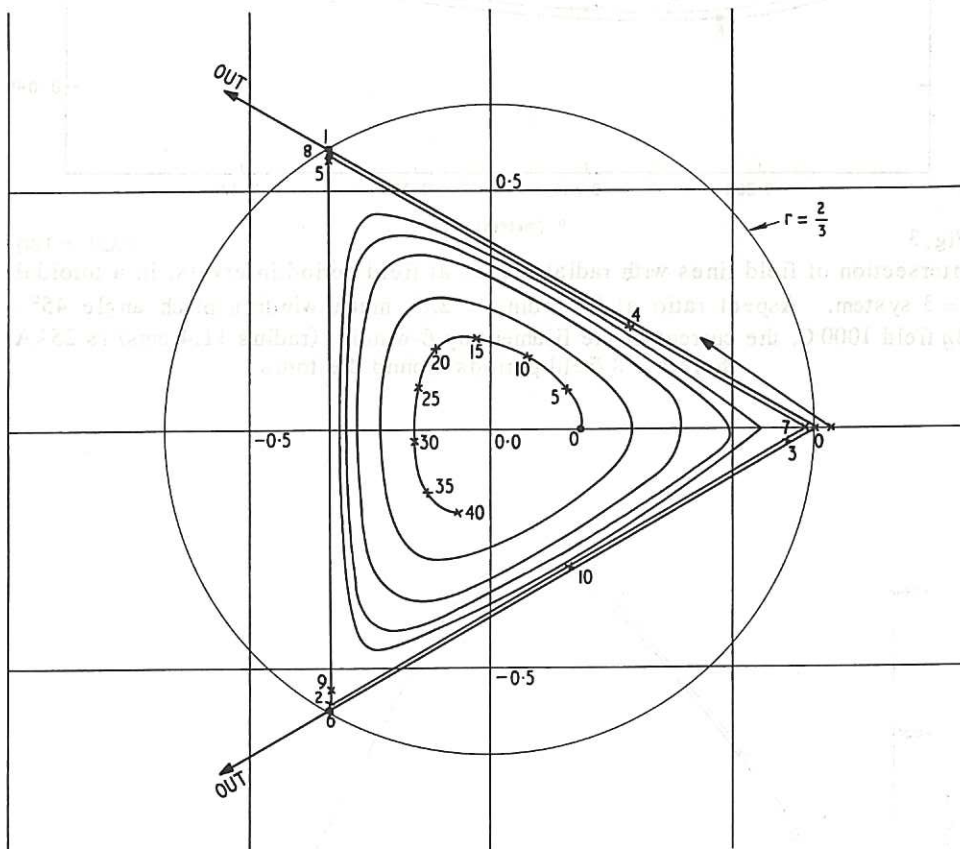


Fig. 2 (CLM-P 129)  
 The intersection of field lines with z-planes at intervals of one field period in a straight analytic field with helical symmetry. The planes are numbered consecutively and the numbers corresponding to some of the intersections are shown

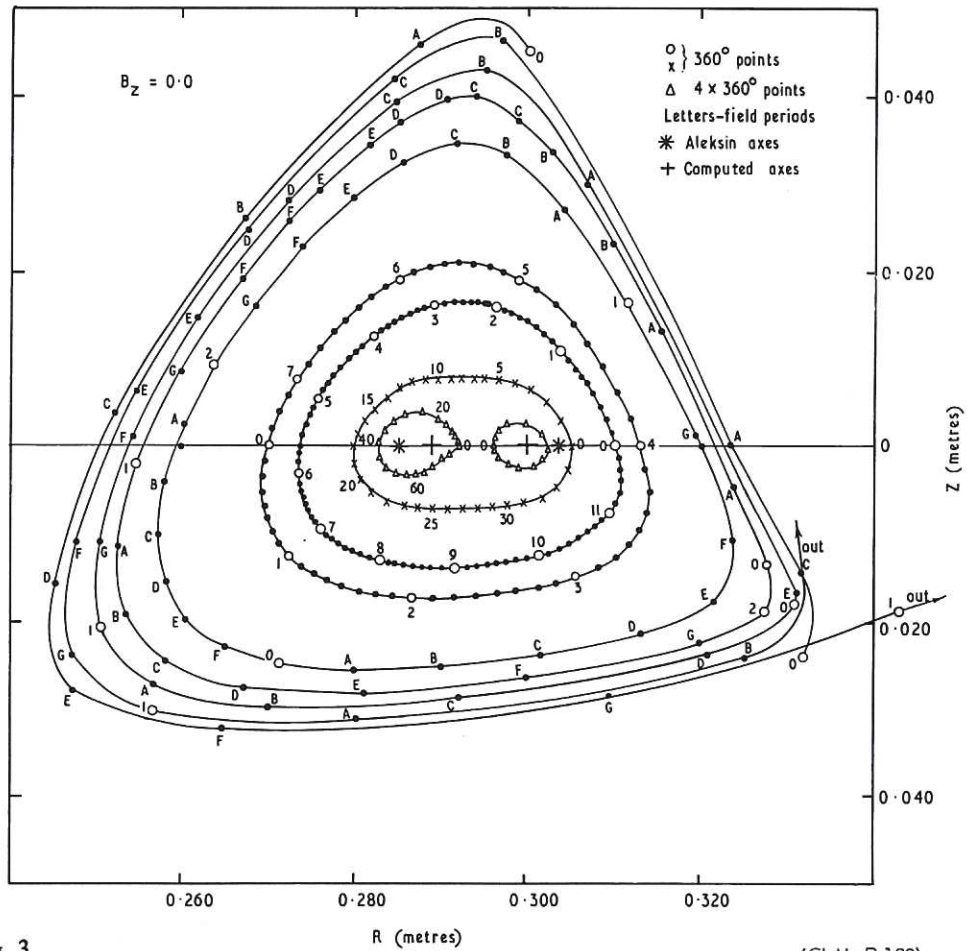


Fig. 3 (CLM-P 129)  
 Intersection of field lines with radial planes at field period intervals, in a toroidal  $\ell = 3$  system. Aspect ratio at  $\ell$ -winding = 2.8, mean winding pitch angle  $45^\circ$ ,  $B_\theta$  field 1000 G, the current in the filamentary  $\ell$ -winding (radius 11.4 cms) is 25 kA, there are 8 field periods around the torus

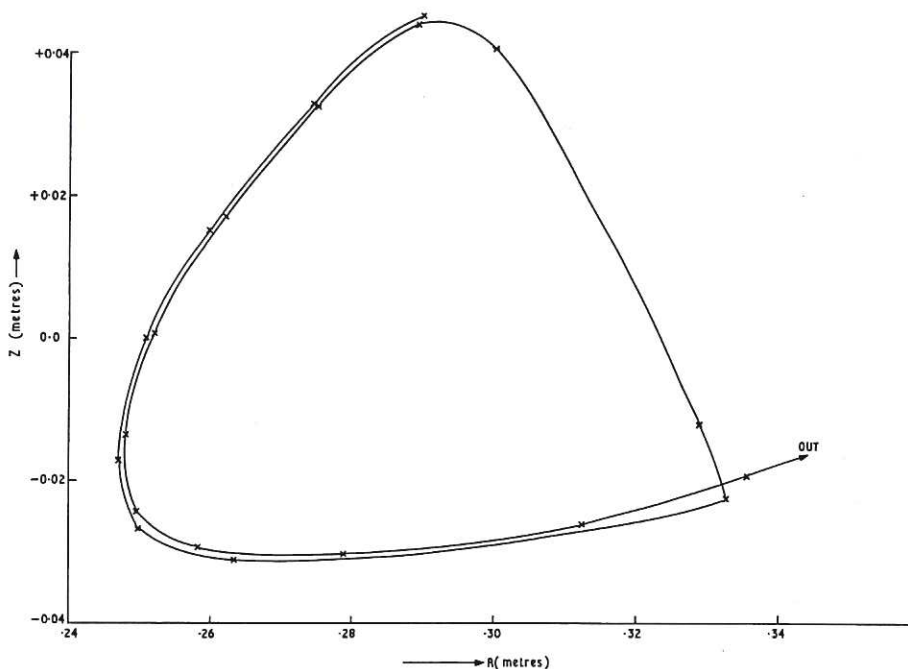


Fig. 4 (CLM-P 129)  
 An outer surface of Fig. 3 showing complex structure

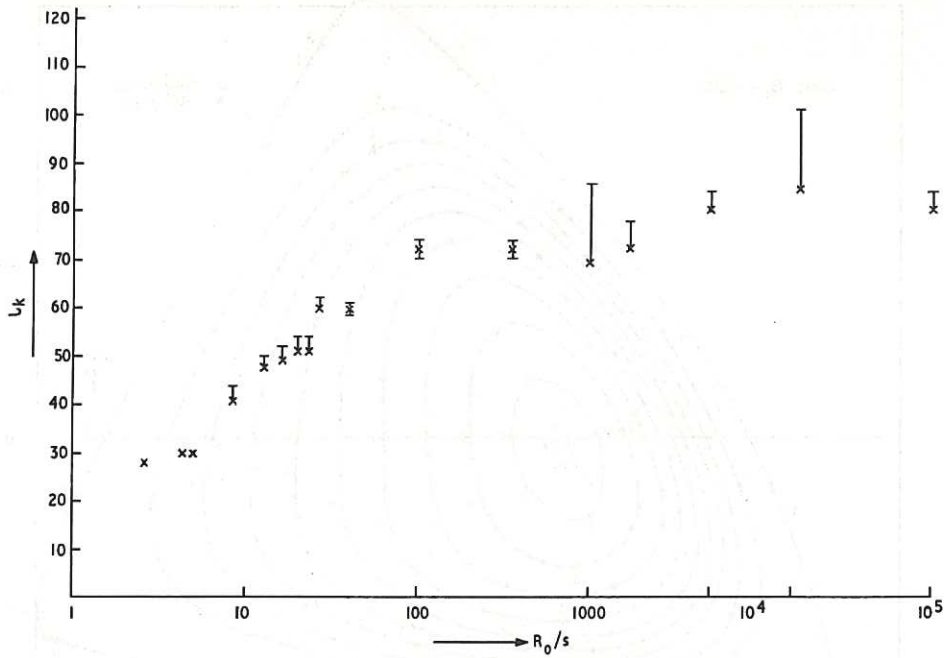


Fig. 5 (CLM-P 129)  
 Variation of rotational transform on last closed surface as a function of aspect ratio at the  $\ell$ -winding. Mean winding pitch angle  $45^\circ$

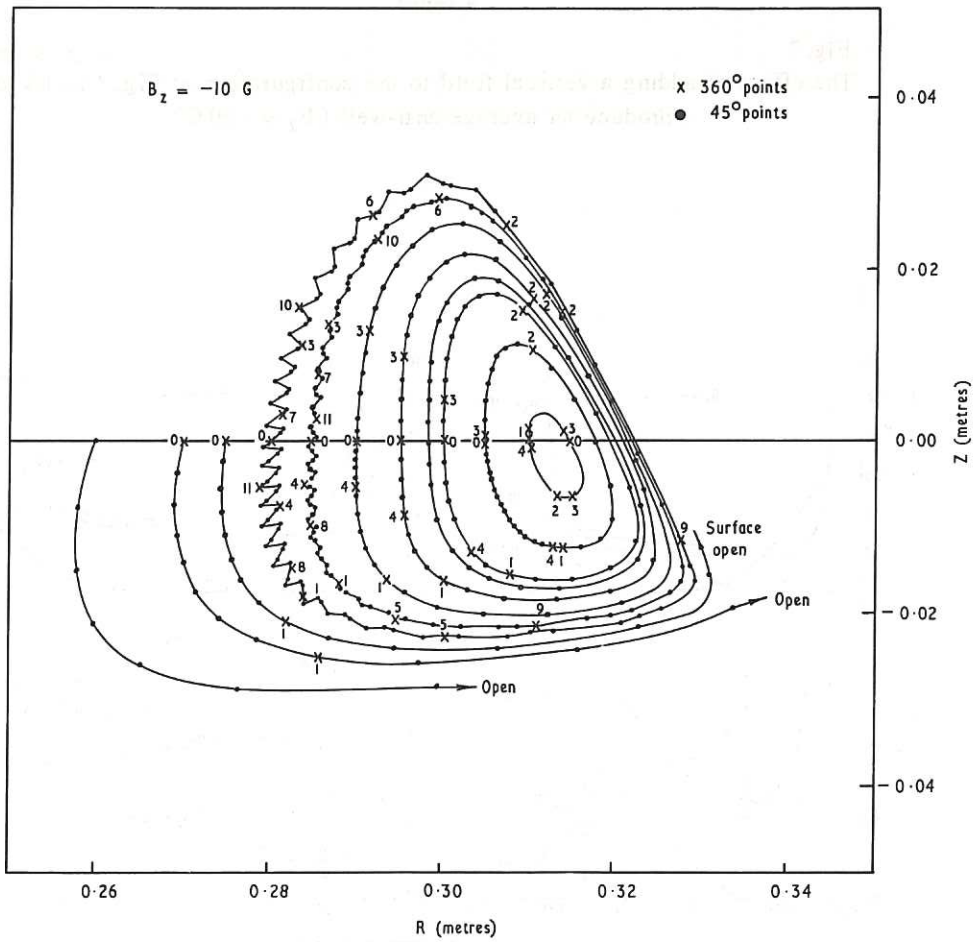


Fig. 6 (CLM-P 129)  
 The effect of adding a vertical field to the configuration of Fig. 3 so as to produce an average magnetic well ( $B_z = -10$  G)

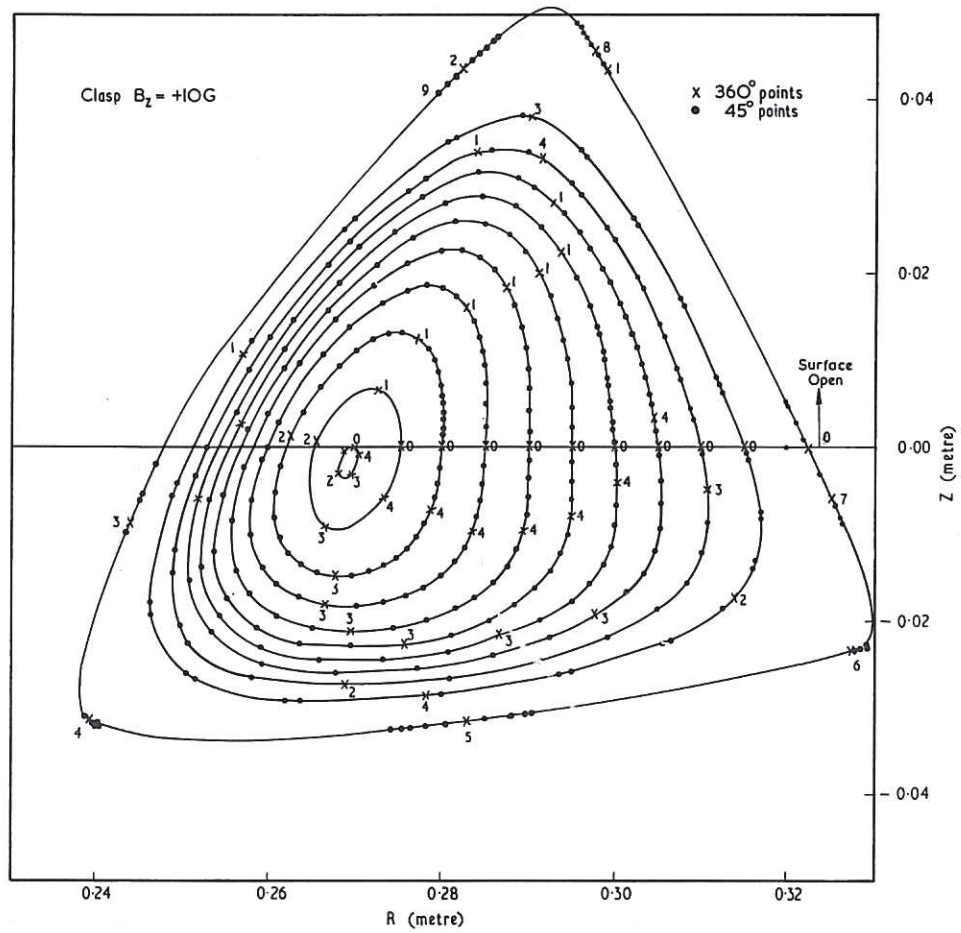


Fig. 7 (CLM-P 129)  
 The effect of adding a vertical field to the configuration of Fig. 3 so as to produce an average anti-well ( $B_z = +10$  G)

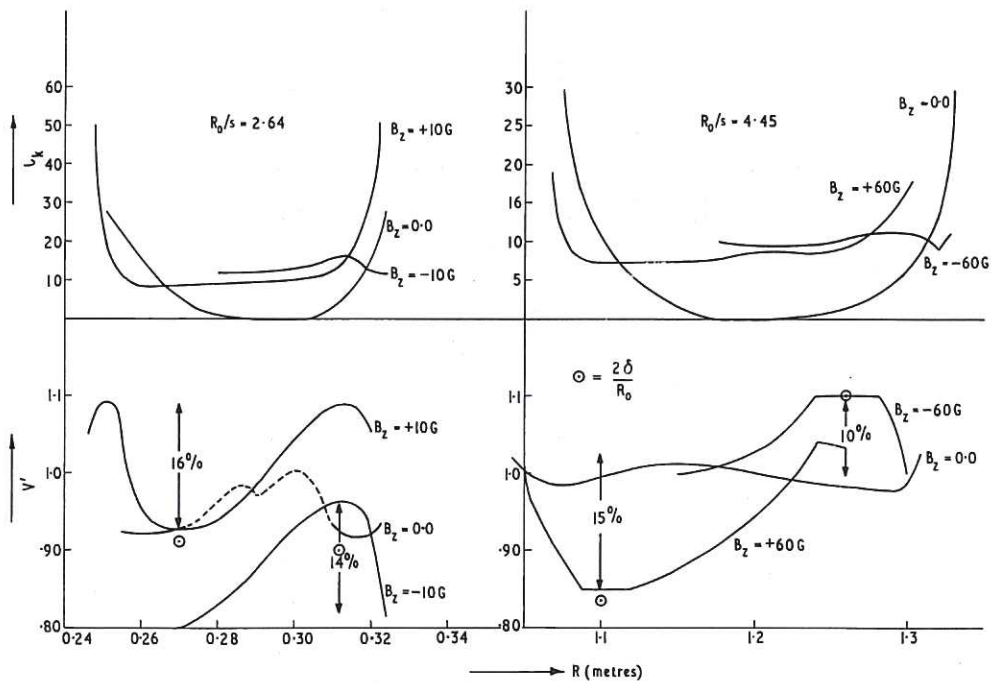


Fig. 8 (CLM-P 129)  
 The variation of  $l_k$  and  $V'$  across the horizontal plane of symmetry

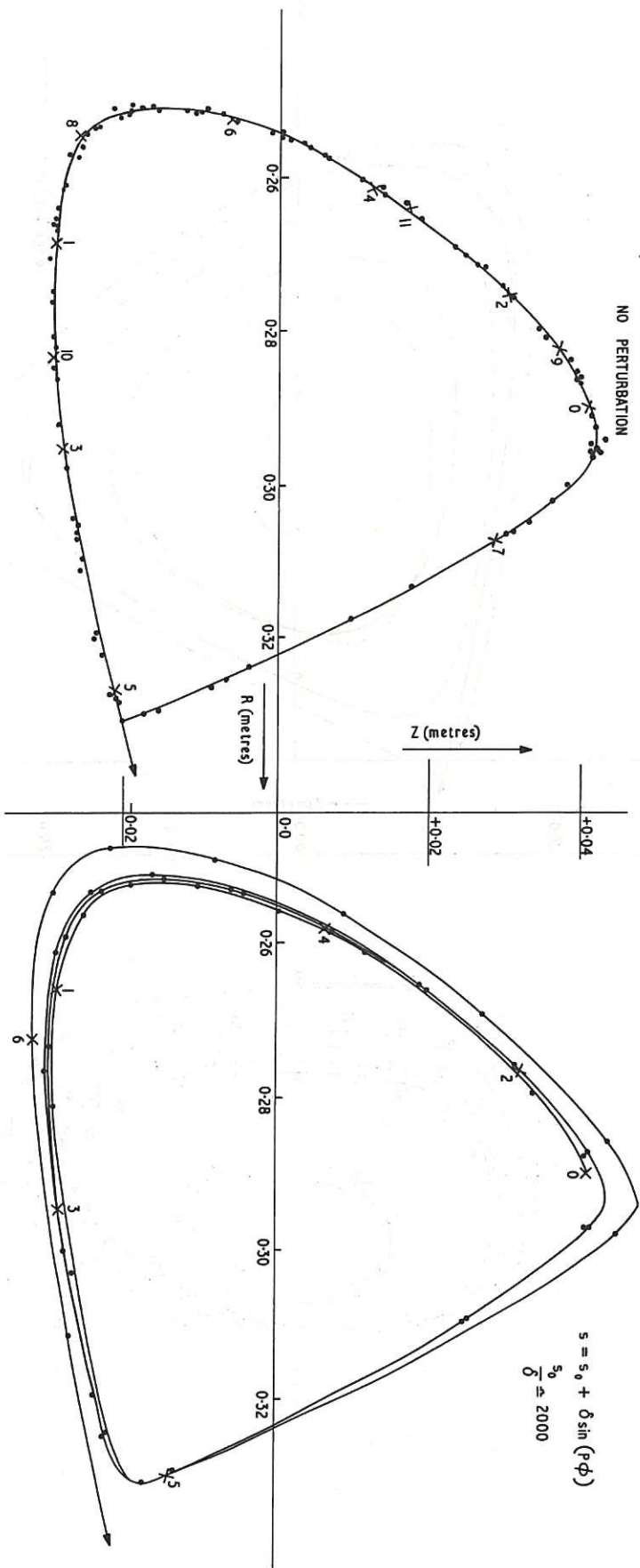
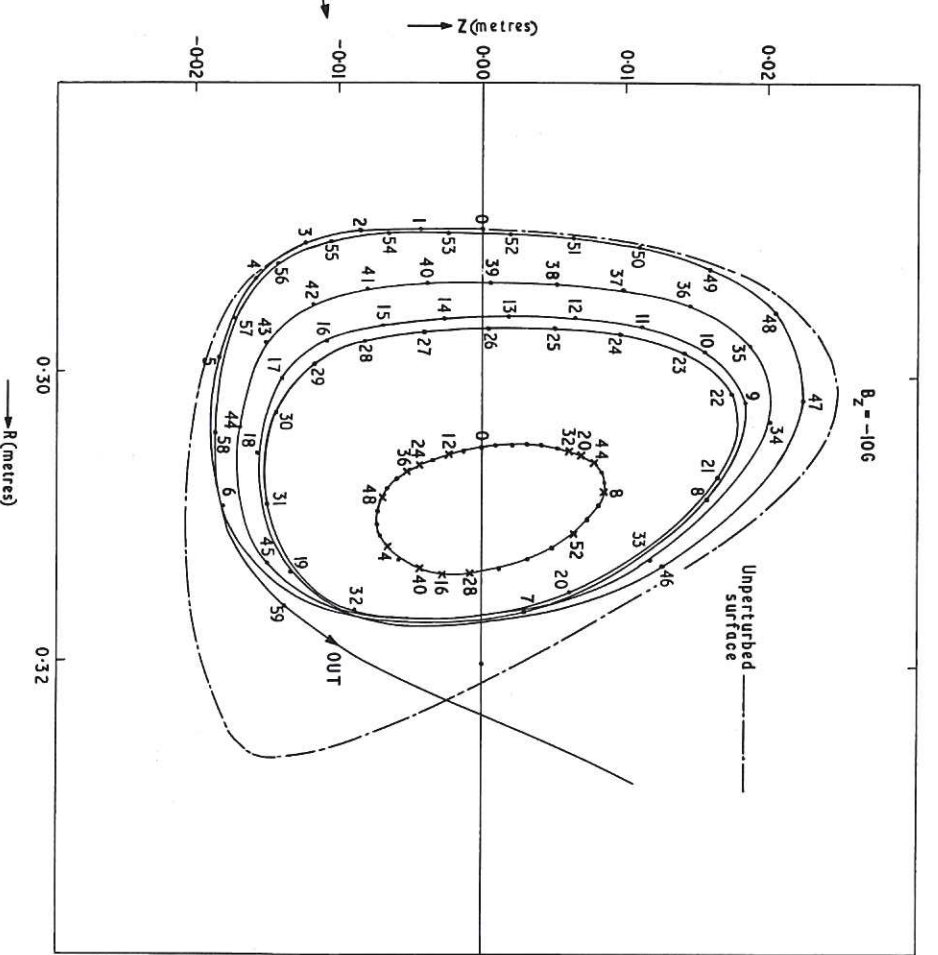
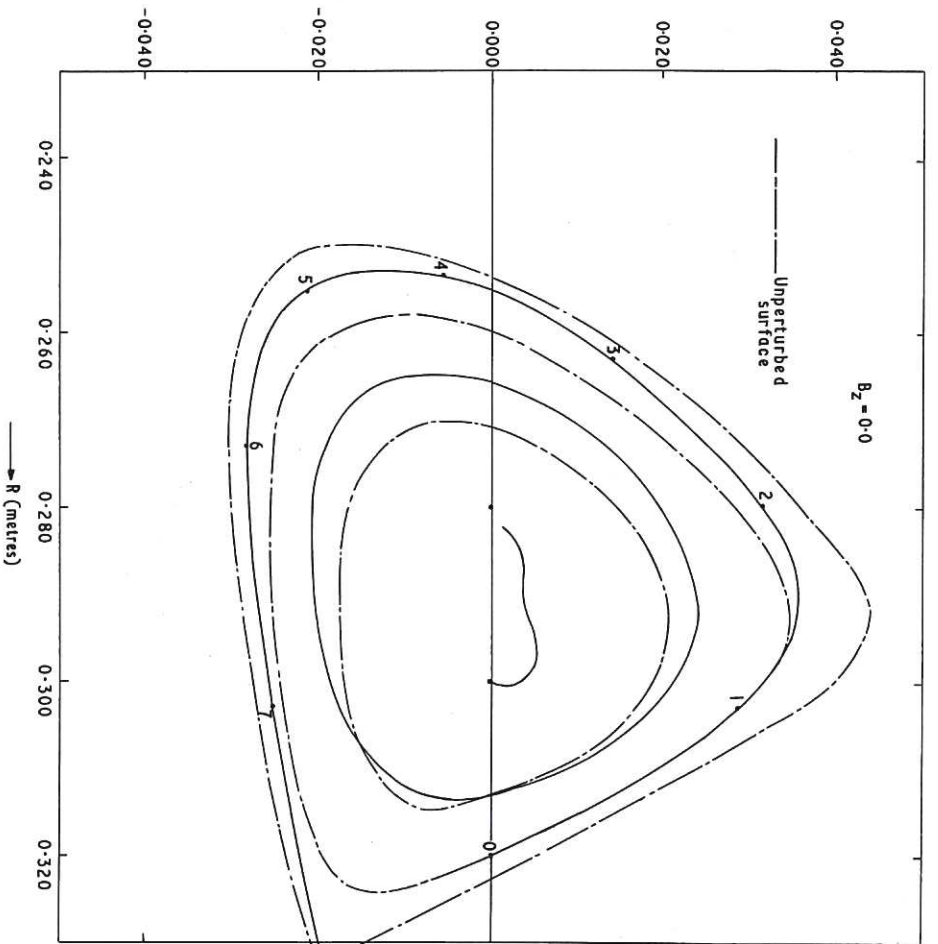


Fig. 9  
 The effect of a small resonant error in the  $l$ -winding minor radius  
 (CLM-P129)



**Fig. 10**  
 The effect of larger resonant perturbations. Points are plotted in the radial planes in which the positive perturbation loops occur. Surfaces in the unperturbed field are shown for comparison (CLM-P 129)

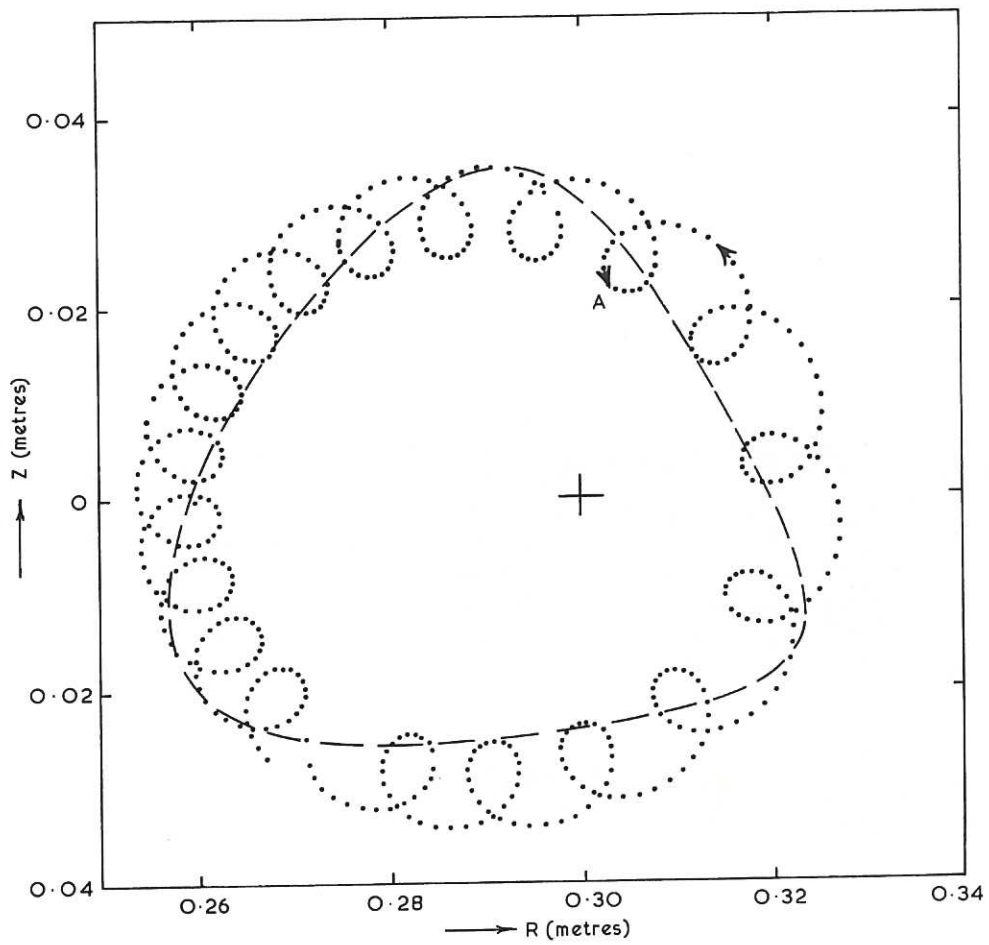


Fig. 11 (CLM - P 129)  
 The trajectory of a field line in the R-Z plane. Note that the intersections of the  $\ell$ -winding with this plane rotate anti-clockwise about the axis as we move along the circular axis





